Engineering the Glass Structure of a Discotic Liquid Crystal by Multiple Kinetic Arrests

Junguang Yu,¹ Zhenxuan Chen,¹ Caroline Fatina,¹ Debaditya Chatterjee,² Harald Bock,³ Ranko Richert,⁴ Paul Voyles,² M. D. Ediger,⁵ Lian Yu¹,*

ABSTRACT. X-ray scattering has been used to characterize the columnar packing and the π stacking in a glass-forming discotic liquid crystal. In the equilibrium liquid state, the intensities of the scattering peaks for π stacking and columnar packing are proportional to each other, indicating concurrent development of the two orders. Upon cooling into the glassy state, the π - π distance shows kinetic arrest with a change of the thermal expansion coefficient (TEC) from 321 ppm/K to 109 ppm/K, while the intercolumnar spacing exhibits a constant TEC of 113 ppm/K. By changing the cooling rate, it is possible to prepare glasses with a wide range of columnar and π stacking order, including zero order. For each glass, the columnar order and the π stacking order correspond to a much hotter liquid than its enthalpy and π - π distance, with the difference between the two internal (fictive) temperatures exceeding 100 K. By comparison with the relaxation map obtained by dielectric spectroscopy, we find that the δ mode (disc tumbling within a column) controls the columnar order and the π stacking order trapped in the glass, while the α mode (disc spinning about its axis) controls the enthalpy and the π - π spacing. Our finding is relevant for controlling the different structural features of a molecular glass to optimize its properties.

Corresponding author: lian.yu@wisc.edu

¹ School of Pharmacy, University of Wisconsin-Madison, Madison, WI 53705, USA

² Department of Materials Science and Engineering, University of Wisconsin-Madison, Madison, WI 53705, USA

³ Centre de Recherche Paul Pascal - CNRS & Université de Bordeaux, 33600 Pessac, France

⁴ School of Molecular Sciences, Arizona State University, AZ 85287, USA

⁵ Department of Chemistry, University of Wisconsin-Madison, Madison, WI 53705, USA

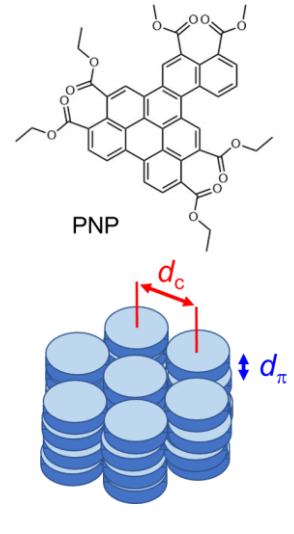
INTRODUCTION

A glass is formed by cooling a liquid while avoiding crystallization. At the glass transition, a flowing liquid hardens to a solid. As materials, glasses provide liquid-like macroscopic homogeneity, ability to dissolve multiple components in a single phase, ease of processing (e.g., drawing fibers), and higher solubility than crystals. A limitation in traditional glass fabrication, however, is that each glass has one liquid phase as precursor and thus a narrow range of structures. In contrast, crystal polymorphs are often exploited as a tool for structural modification in crystal engineering. It is desirable to develop similar capabilities in glass engineering.

Glass-forming liquid crystals (LC) provide an opportunity to systematically control the structure of glasses. Molecules in a LC can be highly ordered in the fluid state and that order can be frozen in a glass. He cent work has shown that LC order is not only *transferable* to a glass but also *tunable* by adjusting the cooling rate. For the calamitic LCs itraconazole and saperconazole, this approach enabled preparation of glasses with smectic order ranging from strong to none. Similarly, for the discotic LC phenanthro[1,2,3,4-ghi]perylene-1,6,7,12,13,16-hexacarboxylic 6,7,12,13-tetraethyl,1,16-dimethyl ester (PNP, Scheme 1), it is possible to prepare glasses with strong and zero columnar order. In both cases, the amount of LC order in the glass is determined by the kinetic arrest of a slow relaxation mode (end-over-end rotation for rods and heads-overtails flip for discs?). This relaxation mode is frozen at a higher temperature than the other degrees of freedom, producing a glass with multiple internal (fictive) temperatures for its different structural features. Given the common occurrence of multiple relaxation modes in calamitic 6, 8, 10, 11 and discotic LCs, 7, 12-16 this phenomenon may have general relevance

for understanding the structures of their glasses.

In this work, we investigate the glass structures of the discotic LC (DLC) former PNP with particular attention to the π stacking order and its dependence on glass-forming conditions. DLCs have attracted attention for their potential applications in organic electronics. ¹⁷⁻²⁰ The system studied here, PNP, has been synthesized to have a glassy columnar LC phase at room temperature for electronic applications. ²¹ Chen *et al.* have investigated the effect of cooling rate on the columnar order of a PNP glass, ⁷ and we focus here on the π stacking order and its relation to the columnar order. As illustrated in Scheme 1, the columnar order refers to the organization of the discotic molecules into regularly arranged columns and the π stacking order to the regular face-to-face contact of the aromatic cores. The π stacking order is of interest because DLCs can provide enhanced conductance along the columnar axis²² and improved overlap of the π orbitals can improve conductance. ^{19, 23}



Scheme 1. Molecular structure of PNP (top) and the two mesoscopic orders (columnar and π stacking) studied here (bottom).

An interesting question concerning glass-forming LCs is the nature of their glass transition. Given the common description of a LC as having crystal-like order in some dimensions and liquid-like order in others, will a glass transition influence the two dimensions differently? For a triphenylene-based DLC, the intercolumnar spacing is less affected by the glass transition than the intracolumnar spacing,³¹ but for the calamitic LC itraconazole⁹ and saperconazole,⁶ the glass transition has strong influence on both the structure of the smectic layers and the packing within each layer. This question is relevant for understanding the glass structures of LCs and will be investigated for PNP.

We find that by varying the cooling rate, PNP glasses can be prepared with widely different π stacking order and columnar order, including zero order. In the equilibrium liquid state, the intensities of the scattering peaks for π stacking and for columnar packing are proportional to each other, indicating concurrent development of the two orders. On entering the glassy state, the π stacking distance undergoes kinetic arrest with a 3-fold reduction of the thermal expansion coefficient (TEC), while the TEC associated with intercolumnar spacing remains constant. Upon cooling, the columnar order and the π stacking order are frozen at the kinetic arrest temperature of the δ relaxation mode (disc tumbling), while the π stacking distance and enthalpy freeze at the kinetic arrest temperature of the α relaxation (rotation about the column axis). We discuss the relevance of our result for controlling the structural features of a glass to optimize its properties.

EXPERIMENTAL SECTION

Materials and Sample Preparation. Phenanthro[1,2,3,4-ghi]perylene-1,6,7,12,13,16-hexacarboxylic 6,7,12,13-tetraethyl1,16-dimethyl ester (PNP) was synthesized using the procedure of Kelber et al. Crystalline PNP powder was filled into an X-ray transmitting capillary tube (Charles Supper, MA, 1.5 mm OD, 10 μm wall thickness) and melted before flame sealing the tube. A glass sample was prepared by heating the sample above the LC clearing temperature (519 K) and cooling the isotropic liquid at a controlled rate (R_c). Slower cooling was performed by programed cooling in a DSC cell and faster cooling by cooling a sample preheated to 550 K in ambient air or in an ice-water bath. In the latter case, the cooling rate was measured by performing the same cooling procedure with a thermocouple coated with a 1.5 mm layer of epoxy to mimic the thermal conductivity of the sample.

X-Ray Scattering. X-ray scattering was measured with a Bruker D8 Discover diffractometer equipped with a Cu Kα source ($\lambda = 1.5406$ Å), a Vantec 500 area detector, and an Instec mK2000 heating stage. Temperature was calibrated using the melting points of crystals (Benzamide, 401 K; D-mannitol Form β, 439 K; Griseofulvin Form I, 493 K) and PNP's clearing temperature (519 K). The sample in a capillary tube was irradiated perpendicularly and the scattered X-ray was measured in the transmission geometry. The area detector was placed off-center at $2\theta = 20^{\circ}$ and 20 cm from the sample to allow coverage of the $q = 4\pi \sin \theta/\lambda$ range from 0.3 to 2.1 Å⁻¹ and simultaneous measurement of the columnar and the π - π scattering. Griseofulvin Form I and silver

behenate were used to calibrate the diffraction angle and to determine the instrumental resolution. Each glass sample was measured during heating and after reaching the liquid state, measured during cooling. At each measurement temperature, the sample was equilibrated for 5 min and measured for 5 min. The two-dimensional X-ray scattering data was integrated using the software Datasqueeze²⁴ to yield a one dimensional intensity vs q plot.

Differential Scanning Calorimetry (DSC). A TA Q2000 Differential Scanning Calorimeter was used to measure the relative enthalpies of different glasses. Each sample (3–5 mg) was placed in a crimped aluminum pan and analyzed under 50 mL/min N₂ purge. For each measurement, the sample was cooled at a controlled rate (1–30 K/min) from 538 K (isotropic state) to 303 K (glassy state) and heated at 10 K/min to 538 K.

RESULTS AND DISCUSSION

 π Stacking Order and Columnar Order in the Equilibrium Liquid State. Figure 1 shows the typical X-ray scattering data collected during cooling from an isotropic liquid of PNP. The instrument setup allowed simultaneous measurement of the columnar scattering peak and the π - π

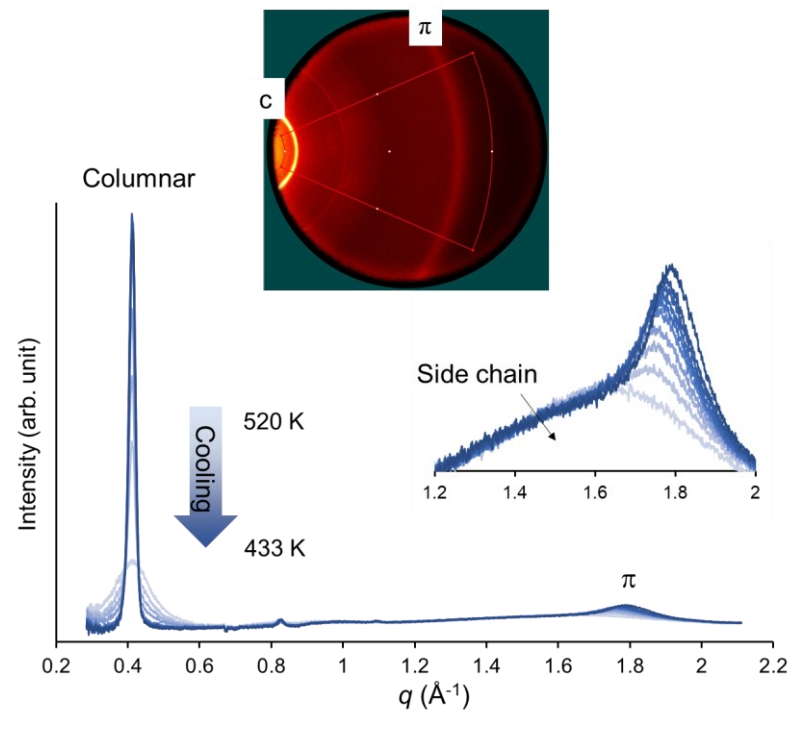


Figure 1. X-ray scattering curves of PNP measured during cooling from the isotropic liquid state. The 0.41 Å⁻¹ peak results from intercolumnar scattering, the 1.8 Å⁻¹ peak from π - π scattering, and the broad feature near 1.5 Å⁻¹ from the correlation between the side chains of the aromatic core. Insets: a typical 2D scattering pattern and an enlarged view of the π scattering peak.

scattering peak; see a typical 2D scattering image in the inset where the two peaks are labeled c and π . The 2D scattering pattern consists of concentric rings, indicating no preferred orientation of LC domains. Azimuthal integration of the 2D pattern yielded the intensity vs. q curves in the main figure, where q is the magnitude of the momentum transfer.

With cooling below the isotropic-columnar transition temperature ($T_c = 519 \text{ K}$), peaks emerge at $q_c = 0.41 \text{ Å}^{-1}$ and $q_\pi = 1.8 \text{ Å}^{-1}$. The peak at q_c results from the scattering by the regularly arranged columns²¹ and the peak at q_π from the regular stacking of the aromatic cores (π stacking);^{25,28} see Scheme 1. From these peak positions we obtain $d_c = 2\pi/q_c = 15.4 \text{ Å}$ for the intercolumnar distance and $d_\pi = 2\pi/q_\pi = 3.5 \text{ Å}$ for the π - π stacking distance. In addition to these two peaks, a broad peak is observed to the left of the π stacking peak near 1.5 Å⁻¹ and attributed to the correlation of the side chains attached to the aromatic core.²⁵ Figure 1 shows that with cooling below T_c , the columnar peak and the π stacking peak grow simultaneously, indicating that the two structural orders increase together. Furthermore, the π stacking peak is significantly broader than the columnar peak, indicating a shorter correlation length. Below we analyze these results quantitatively with aid of curve fitting.

An X-ray scattering peak provides information on the underlying molecular packing giving rise to the peak: the average atomic spacing from the peak position (d = $2\pi/q$), the correlation length from the peak width, and the correlation strength (number of correlated atoms) from the peak area. To obtain these parameters, peaking fitting was performed to isolate each scattering peak. As shown in Figure 2, the signal near 0.41 Å⁻¹ is well described as a sum of a sharp Gaussian and a broad Lorentzian. The broader Lorentzian results from the excluded volume effect²⁶ where each molecule orders its neighbors through its disc-like shape even in the isotropic liquid state $(T > T_c)$ and the sharper Gaussian is used to quantify the columnar order in the LC phase.²⁷ Figure 2b shows that the signal near 1.8 Å⁻¹ is well described as a sum of two Lorentzians, with the broader component at 1.5 Å^{-1} describing the correlation of the side chains of the aromatic cores and the sharp component at 1.8 Å⁻¹ the π stacking order.^{25,28}

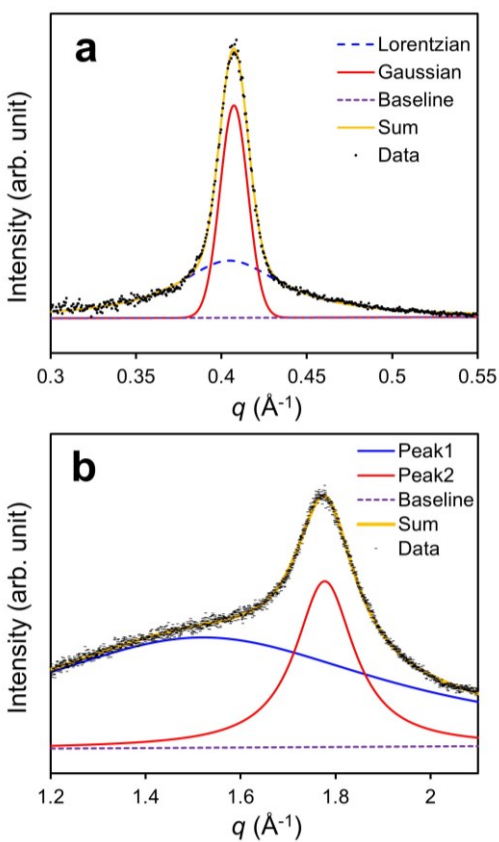


Figure 2. Fitting of (a) the columnar peak and (b) the π stacking peak.

Figures 3, 4, and 5 present the positions, the widths, and the areas of the columnar and π scattering peaks as functions of temperature. As shown in Figure 3a, on cooling below the clearing temperature T_c , the columnar peak position q_c increases almost linearly with temperature with a nearly constant TEC, $\alpha_c =$ 113 ppm/K, in good agreement with Chen et al.'s value of 117 ppm/K.⁷ The temperature range studied spans the glass transition temperature $T_{\rm g}$ detected by DSC (393 K) and $q_{\rm c}$ is insensitive to the passage through $T_{\rm g}$. The second y axis in Figure 3a shows the intercolumnar spacing, $d_c = 2\pi/q_c$, which decreases with cooling from 15.4 Å to 15.1 Å in the temperature range studied. In contrast to the temperature dependence of q_c , the π stacking peak position q_{π} is sensitive to the passage through T_g : its TEC decreases from α_{π} = 321 ppm/K above T_g to α_{π} = 107 ppm/K below, a drop by a factor of 3. From α_c and α_{π} , the volumetric TEC can be calculated, $\alpha_v = 2\alpha_c$ + α_{π} , yielding α_{v} = 547 ppm/K above T_{g} and 333 ppm/K below. A change of TEC across $T_{\rm g}$ is a hallmark of a liquid's glass transition.^{29, 30} PNP's TECs indicate that its glass transition is associated mainly with the intracolumnar

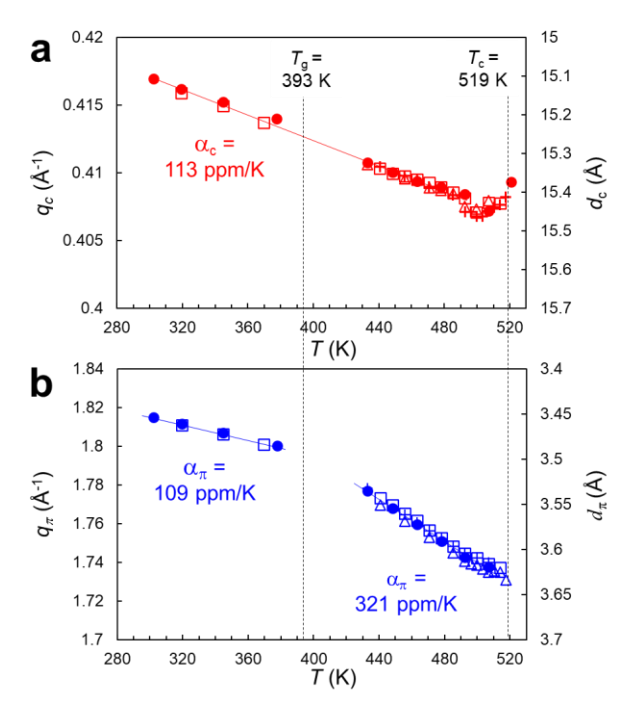


Figure 3. Temperature dependence of the positions of (a) the columnar peak q_c and (b) the π stacking peak q_π during cooling from the isotropic liquid state. The different symbols indicate different datasets. q_c is insensitive to the passage through T_g (393 K), but q_π is. The range 393 – 420 K was bypassed due to crystallization. α_c and α_π are the thermal expansion coefficients (TECs) for the intercolumnar spacing and the π - π spacing, respectively.

structure, not the intercolumnar spacing. During cooling, the system is crystal-like throughout the glass transition with respect to d_c but shows a glass transition in d_π . This behavior is analogous to that of a triphenylene-based DLC³¹ where α_c decreases linearly with cooling through T_g , while α_π shows a steplike drop at T_g . This result is sensible in reference to the common view that a columnar LC has crystal-like intercolumnar packing and liquid-like intracolumnar packing, but is in contrast to the behavior of the calamitic LC itraconazole⁹ for which the glass transition influences the TECs of both the spacing between smectic layers and the distance between molecules within a layer.⁹ The literature on DLCs shows diverse thermal expansion behaviors with the α_c values ranging from positive^{31,ADD} Grigoriadis et al. Adv. Mater. 22, 1403-1406 (2010) to negative²⁵ and from being larger in amplitude than α_π ADD Grigoriadis et al. Adv. Mater. 22, 1403-1406 (2010) to smaller.³¹ Relative to this range, the thermal expansion of PNP is not exceptional.

Figure 4 shows the full widths at half maximum (FWHM) of the columnar peak and the π stacking peak as functions of temperature. The columnar peak is much sharper than the π stacking peak and in fact, is limited by the instrumental resolution (FWHM = 0.016 Å^{-1} , obtained by Gaussian fitting of crystalline peaks and shown in Figure 4 as the horizontal line). The width of the π stacking peak, in contrast, exceeds the instrumental resolution, allowing calculation of its correlation length ξ . A Lorentzian scattering peak corresponds in real space to an exponentially damped sinusoidal pair-correlation function with a decay length of $\xi = 2/\text{FWHM}.^9$ Upon cooling from T_c , the FWHM

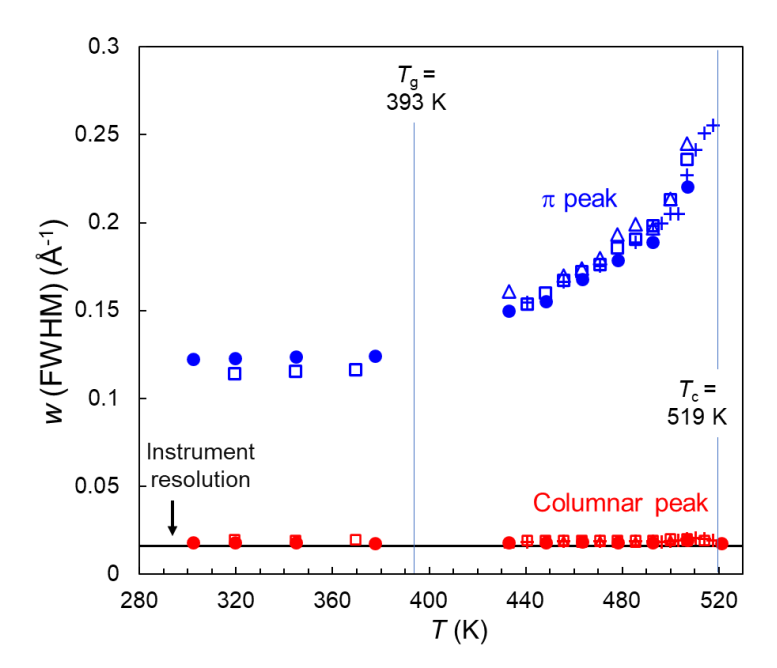


Figure 4. Widths (FWHM) of the columnar peak and the π stacking peak vs. temperature during cooling from the isotropic liquid.

of the π stacking peak decreases from 0.25 Å⁻¹ to 0.12 Å⁻¹ near and below $T_{\rm g}$; this translates to a doubling of the correlation length from 8 Å to 17 Å (2 to 5 discs). Below $T_{\rm g}$, ξ is insensitive to temperature, as expected. These correlation lengths are relatively short, only slightly longer than that for the non-mesogen glycerol near $T_{\rm g}$, $\xi \approx 8$ Å.²⁹ The short correlation length for PNP's intracolumnar structure is consistent with a confined, one-dimensional liquid that exhibits a glass transition (Figure 3b). For a hexa-*peri*-hexabenzocoronene (HBC)-based DLC, Hansen *et al.*¹³ observed similarly short intracolumnar correlation length (24 Å or 7 discs) and associated it with a heterogeneous columnar structure containing segments of well-packed discs separated by disordered regions. It would be of interest to learn if PNP has a similar or a different structure.

Figure 5a shows the temperature dependence of the areas of the columnar peak A_c and the π stacking peak A_π . Both A_c and A_π rise sharply with cooling below T_c and evolve more slowly below 480 K. Below 480 K, A_c appears to decrease slightly, while A_π appears to increase slightly. In Figure 5b, the two areas are plotted against each other, and we observe an approximately proportional relation, indicating that the two types of order grow roughly in proportion. This result is sensible since better organized, tightly packed columns are expected to organize the discs within each column. It is unclear why the two orders evolve somewhat differently below 480 K. Given that each scattering peak is isolated by curve fitting from an overlapping peak (Figure 2), model accuracy plays a role. This effect, if real, could reflect the different responses of the inter- and intracolumnar structures to the glass transition (Figure 3): while the intercolumnar spacing shows no kinetic arrest, the π - π spacing does. Thus, during cooling below T_g , the intracolumnar structure could exhibit a slight glass aging effect (evolving toward equilibrium), while the intercolumnar structure might not. The calamitic LC itraconazole shows a slight decrease of smectic order with

cooling in the glassy state,⁵ which was related to the tension that developed in the glass due to the mismatch of the thermal expansion coefficients of itraconazole and its container.

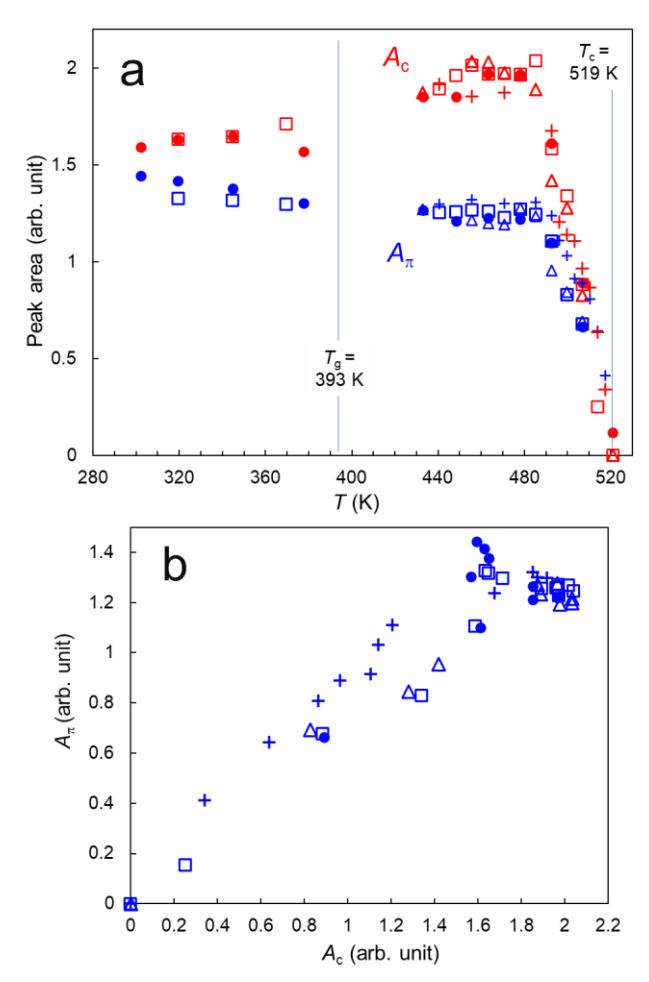


Figure 5. Temperature dependence of the areas of the columnar peak A_c and the π stacking peak A_π during cooling from the isotropic liquid state. The different symbols correspond to different datasets. The two orders rise together below T_c and stabilize near 480 K.

Structures of PNP Glasses Prepared at Different Cooling Rates. We now turn to the effect of

cooling rate on the different structural features of a PNP glass. Figure 6 shows the X-ray scattering patterns of PNP glasses prepared by cooling at different rates. The glass prepared at the lowest cooling rate (0.5 K/s) had the highest columnar order and the π stacking order, while faster cooling reduced both orders in the glass. Given the two orders correlated are strongly in equilibrium liquid state (Figure 5b), it is not surprising to observe this qualitative result. But as we show below by quantitative analysis, the two orders show significant decoupling that is relevant for controlling the π stacking in the glassy state.

To quantify the structure of a glass, we adopt the standard measure of fictive temperature $T_{\rm f}$. For a liquid in equilibrium, $T_{\rm f}$ is equal to the actual temperature; for an out-of-equilibrium glass, T_f is higher than the actual temperature, corresponding to an equilibrium liquid that would display the same structural feature (e.g., enthalpy and volume) aside from the thermal-expansion effect. Figure 7 illustrates the determination of $T_{\rm f}$ for two structural features in a single PNP glass, 9 namely, the π - π spacing d_{π} (= $2\pi/q_{\pi}$) and the π stacking order measured by the π scattering peak area A_{π} . This glass was prepared by cooling at 20 K/s and its Xray scattering was measured during heating from the glassy state to the liquid state (open symbols). The solid symbols indicate the equilibrium liquid behavior observed during cooling from the isotropic state (Figures 3 and 5). Figure 7a shows that as the glass was heated, d_{π} increases linearly in the glassy state $(T < T_g)$ and on entering the liquid state $(T > T_g)$, increases at a faster rate. A difficulty in this measurement is that above $T_{\rm g}$, the sample crystallized from the nuclei formed at low

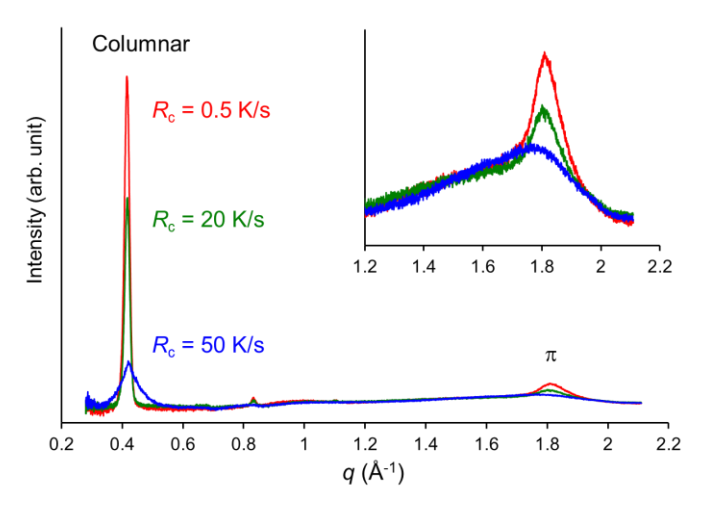


Figure 6. X-ray scattering patterns of PNP glasses prepared by cooling at different rates and measured at 298 K.

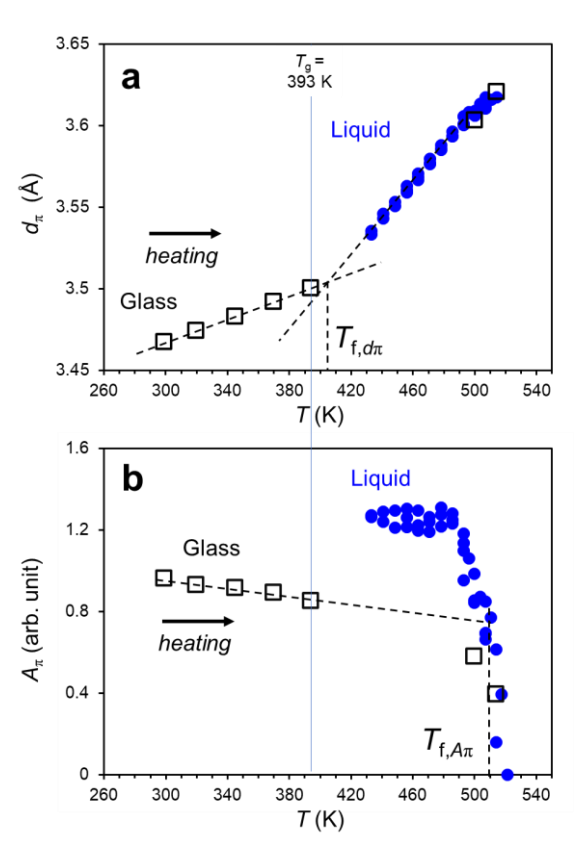


Figure 7. Fictive temperature $T_{\rm f}$ of a PNP glass with respect to two features of π stacking: (a) π - π spacing d_{π} and (b) area of the scattering peak A_{π} . The glass was prepared by cooling at 20 K/s and measured during heating (open square). $T_{\rm f}$ is the intersection of the glass line and the liquid line (solid symbols).

temperature, causing a gap in the data, and the measurement could resume only after the crystals melted near 490 K. (Crystallization was less of a problem when cooling a liquid from high temperature.) Nevertheless, the glassy-state and the liquid-state data can be combined to obtain the fictive temperature T_f (Figure 7a) at the intersection of the glass line and the liquid line. For this glass, $T_f = 405$ K with respect to d_{π} . In Figure 7b, a similar procedure is used to determine the T_f with respect to the peak area A_{π} , yielding $T_f = 509$ K. Thus, for this glass, the T_f for A_{π} is much higher than that for d_{π} , by more than 100 K. These two structural features both characterize the π stacking in a PNP glass but its different aspects, namely, the molecular spacing (d_{π}) and the number of correlated molecules (A_{π}) . The large difference between the two fictive temperatures indicates that during cooling, the two structural features are frozen at very different temperatures.

In Figure 8, we plot the fictive temperatures $T_{\rm f}$ of a PNP glass against the cooling rate $R_{\rm c}$ used to prepare the glass. The fictive temperatures have been measured with respect to different structural features, including the π - π distance d_{π} and the π stacking order A_{π} used in this work (Figure 7) and the enthalpy H and the columnar order $A_{\rm c}$ used by Chen et al. These results are displayed in the upper half of the figure (solid symbols, +, and x) with the cooling rate $R_{\rm c}$ shown on the right y axis. This format of plotting allows comparison of these results with the relaxation times from dielectric spectroscopy (DS) reported previously. Figure 8 shows that the different structural features of a PNP glass fall in two groups in terms of their fictive temperatures: H and H0 in one

group with lower T_f and A_c and A_{π} in the other group with higher $T_{\rm f}$. These two groups of structural features differ in that H and d_{π} are controlled mainly by the nearest-neighbor correlations, whereas A_c and A_{π} by the correlations of a larger group of molecules. Since the rearrangement of the nearest neighbors is expected to be faster than that of a larger group of molecules, it is sensible that H and d_{π} can remain equilibrated during cooling down to a lower temperature than A_c and A_{π} , leading to their different fictive temperatures. Given that A_c and A_{π} are strongly coupled in the equilibrium liquid state (Figure 5), it is not surprising that both are frozen at similar temperatures and have similar $T_{\rm f}$ values. An analogous grouping of properties has observed in the vitrification of the smectic LC itraconazole.9 In this case,

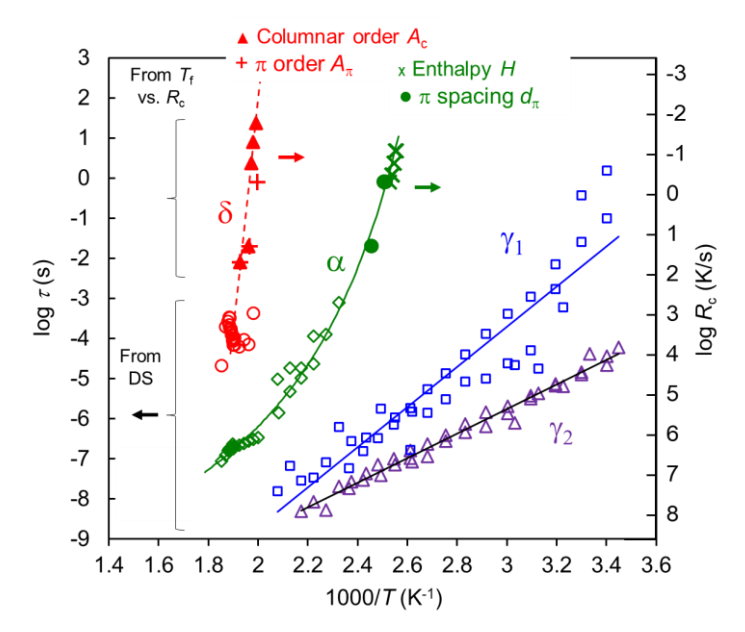


Figure 8. Relaxation map of PNP. Relaxation times from DS (open symbols) are plotted using the left y axis. T_f vs. cooling rate R_c results are plotted using the right y axis. The properties undergoing kinetic arrest are enthalpy (x), columnar order A_c (\triangle), π spacing d_π (\bullet), and π stacking order A_π (+). The two y axes are related by $\tau R_c = C = 0.4$ K.

the smectic order and the correlation length of the intralayer packing are frozen together at a higher temperature, while the enthalpy, the interlayer spacing, and the intralayer spacing freeze together at a lower temperature.

The format of Figure 8 allows comparison of the relaxation times of PNP from DS with those from the kinetic arrest of structural features. The DS-derived relaxation times are shown as open symbols using the left y axis. The two y axes are related by $\tau R_c = C = 0.4$ K, the condition of kinetic arrest obtained previously. PNP has 4 relaxation modes: α , δ , γ_1 , and γ_2 . The α mode is associated with the molecular motions that are kinetically frozen at the DSC T_g . Relative to α , the δ mode is slower and the γ_1 and γ_2 modes faster. The α mode has been assigned to disc rotation about its axis, the δ mode to the disc tumbling within a column, and the γ_1 and γ_2 modes to side chain fluctuations. Figure 8 shows that the kinetic arrest of the different structural features of a PNP glass are associated with the different relaxation modes. The enthalpy H and the π - π spacing $d\pi$ are associated with the $d\pi$ -mode, whereas the columnar order $d\pi$ and the $d\pi$ -matrix stacking order $d\pi$ -are associated with the slower $d\pi$ -mode. This result on PNP echoes the previous result on itraconazole where enthalpy and nearest-neighbor spacing are frozen by the kinetic arrest of the $d\pi$ -relaxation and the regularity of molecular packing is frozen by the kinetic arrest of the $d\pi$ -relaxation of enthalpy fluctuation with the $d\pi$ -relaxation has been observed in molecular liquids without $d\pi$ -and with LC order.

Improving π Stacking Order in the Glassy State. Given the importance of π -orbital overlap in charge mobility, ^{19,23} we consider how the π stacking order can be improved in the glass of a DLC. To maximize charge transport, an ideal structure should have a short π - π distance d_{π} and a long correlation length ξ . According to this work, such a structure should be prepared at a relatively slow cooling rate. Figure 6 shows that the PNP glass prepared at the fastest cooling rate is devoid of any π stacking peak. This is because the molecular motion that controls the development of π stacking (disc tumbling) can be frozen at a high temperature (Figure 8). In addition, Figures 3 and 5 show that during cooling, d_{π} steadily decreases and ξ increases until T_g is reached. This suggests that the most efficient way to improve π stacking is slow cooling through the glass transition region. Slow cooling well above T_g is unnecessary since equilibration is fast; slow cooling well below T_g is unproductive since mobility is slow. Apart from slow cooling through T_g , isothermal aging slightly below T_g could improve π stacking. Based on the result in Figure 3, we expect such aging to reduce d_{π} , but to have little effect on d_g (intercolumnar spacing).

Connection to Vapor-Deposited Glasses. The results presented here provide insight into recent experiments in which glasses of PNP were prepared by vapor-deposition. Bishop *et al.* vapor-deposited PNP glasses at a number of different substrate temperatures and deposition rates, and characterized these materials by X-ray scattering and ellipsometry.³³ At low substrate temperatures or high deposition rates, PNP molecules tended towards "face-on" orientation relative to the

substrate. At high substrate temperatures or low deposition rates, PNP molecules had an "edge-on" orientation and formed hexagonally packed columns that propagate primarily in the plane of the substrate. Bishop *et al.* found that the vapor-deposited PNP glasses had different d_{π} values but that the results could be rationalized by assuming that the surface relaxation process that governs this structure formation slowed by one decade for every 17 K decrease of temperature. Similarly, they reported that the vapor-deposited glasses had different levels of columnar order (in Figure 4 of ref. 22), and that this structural feature could be rationalized with a relaxation process that slowed one decade for every 9 K.³³

There is a striking parallel between the results presented here and those of Bishop $et \, al.$ ³³ In each case, structural order connected with the π stacking distance has a weaker temperature dependence than structural order associated with columnar order. It is reasonable that this correspondence should exist, since faster processes are generally more localized, and more localized relaxation would be expected to be faster whether in the bulk (as in the present work) or at a free surface (as in the work of Bishop $et \, al.$). Based upon this result, we offer the following speculation: If the measures of structural order for the vapor-deposited glasses of a given molecule all show the same temperature dependence (such as the organic semiconductor ABH113³⁴), then we expect that only a single T_f value will be observed for glasses formed by cooling.

Which Aspect of LC Structure Is Influenced by the Glass Transition? A common description of a LC structure is crystal-like order in some dimensions but liquid-like order in others. For a DLC, this view envisions a crystal-like packing of the columns but a liquid-like packing within a column (Scheme 1). Reasoning from this view, one would expect that the glass transition to influence the intracolumnar structure but not the intercolumnar structure. This view is consistent with the DLC of this work (Figure 3) and the DLC of Möller et al.³¹ Both systems show a discontinuous drop of TEC for the π - π spacing upon cooling through $T_{\rm g}$ while the glass transition has less influence on the TEC for intercolumnar spacing. These systems are in contrast, however, to the smectic LC itraconazole. A smectic LC has regular, crystal-like layers that produce sharp X-ray scattering, while its intralayer structure is liquid-like and produces diffuse scattering.³⁵ In this case, one might expect the glass transition to influence the intralayer structure but not the interlayer packing. But for itraconazole, both inter- and intralayer spacings are strongly influenced by the glass transition. It is possible that the different behaviors arise from the different types of liquid crystallinity: 2D hexagonal packing of the columns in the two DLCs vs 1D stacking of layers in itraconazole. For itraconazole, the TEC for the smectic layer spacing is anomalously large (932) ppm/K), suggesting an interdigitation of layers, 9 which would promote a joint response of the interand intralayer structures to the glass transition.

CONCLUSIONS

We have characterized the structures of the equilibrium liquid of the discotic LC PNP and its glasses prepared by cooling at different rates. Attention is paid to the π stacking order because of its importance in charge mobility and device performance. In the equilibrium liquid state, the thermal expansion coefficient (TEC) for the π - π spacing is approximately 3 times that for the columnar spacing and in the glassy state, the two TECs are comparable. The TEC of the columnar spacing is insensitive to the passage through $T_{\rm g}$, whereas the TEC of the π - π spacing decreases by a factor of 3 from above to below $T_{\rm g}$. These results suggest the picture of a "one-dimensional liquid" in which the intercolumnar packing is solid-like and the intracolumnar structure is liquid-like (Figure 3). On cooling below the clearing temperature T_c , the π stacking order (measured by the scattering peak area) grows almost in proportion with the columnar order, reaching a plateau together (Figure 5). By cooling at different rates, glasses can be prepared in which the structural features examined vary significantly (Figure 6). Each glass is characterized by not one, but two fictive temperatures (Figures 7 and 8), with the higher value associated with the columnar order and the π stacking order and the lower value with the enthalpy and the π - π spacing. This is a consequence of the multiple relaxation modes of PNP (Figure 8) with the kinetic arrest of the slow δ relaxation mode defining the columnar and the π stacking order and that of the fast α relaxation mode defining the enthalpy and the π - π spacing.

The finding of this work reinforces the previous conclusion that different aspects of a glass structure can be controlled through the kinetic arrest of the different relaxation modes. This result was first demonstrated with calamitic LCs, and this work extends it to a discotic mesogen. In both cases, the existence of multiple and widely separated relaxation modes leads to the freezing of structural features in separate groups. In both cases, the non-spherical geometry of the molecule is the origin for the different timescales of molecular rotations. The similarity of rod-like and discotic mesogens in this regard suggests a general principle for glass engineering. To optimize a targeted structural feature (e.g., π stacking) in a glass, a processing path should be based on the relaxation mode controlling that feature (Figure 8). For example, to optimize π stacking in PNP, cooling must be slow enough through the T_g of the δ mode, which is well above the conventional T_g of the α mode; otherwise the order may fail to develop. Meanwhile, slow cooling through the conventional T_g helps reduce the π - π spacing (Figure 3) and increase its correlation length (Figure 4).

The state of a glass is often mapped to the equilibrium liquid phase using a fictive temperature $T_{\rm f}$. The difference between $T_{\rm f}$ and the actual temperature is used to indicate how much the glass has fallen out of equilibrium relative to the liquid phase and to model how fast it evolves toward it.*I. M. Hodge, J. Non-Cryst. Solids 169, 211 (1994). https://doi.org/10.1016/0022-3093(94)90321-2 In applying this concept, each glass is usually understood as having a single $T_{\rm f}$. The glass-forming LCs PNP, itraconazole, and saperconazole illustrate the possibility that one glass can have multiple and very different $T_{\rm f}$ values. The origin for this phenomenon is the existence of multiple relaxation modes, whose kinetic arrests occur at different temperatures and freeze different aspects of structure. In principle, the phenomenon can occur for any liquid with multiple relaxation modes. A glass with multiple fictive temperatures has a combination of structural features that is unlike

the equilibrium liquid at any temperature. How such a glass evolves toward equilibrium during aging is an interesting question.

ACKNOWLEDGEMENTS

We thank the NSF (DMR-1904601) for supporting this work and the NSF-supported University of Wisconsin Materials Research Science and Engineering Center (DMR-1720415) for use of its characterization facility.

REFERENCES

- (1) Tsuji, K.; Sorai, M.; Seki, S. New finding of glassy liquid crystal—A non-equilibrium state of cholesteryl hydrogen phthalate. *Bulletin of the Chemical Society of Japan* **1971**, *44* (5), 1452-1452.
- (2) Wedler, W.; Demus, D.; Zaschke, H.; Mohr, K.; Schäfer, W.; Weissflog, W. Vitrification in low-molecular-weight mesogenic compounds. *Journal of Materials Chemistry* **1991**, *1* (3), 347-356.
- (3) Attard, G.; Imrie, C.; Karasz, F. Low molar mass liquid-crystalline glasses: preparation and properties of the. alpha.-(4-cyanobiphenyl-4'-oxy)-. omega.-(1-pyreniminebenzylidene-4'-oxy) alkanes. *Chemistry of materials* **1992**, *4* (6), 1246-1253.
- (4) Chen, S.; Katsis, D.; Schmid, A.; Mastrangelo, J.; Tsutsui, T.; Blanton, T. Circularly polarized light generated by photoexcitation of luminophores in glassy liquid-crystal films. *Nature* **1999**, *397* (6719), 506-508.
- (5) Teerakapibal, R.; Huang, C.; Gujral, A.; Ediger, M. D.; Yu, L. Organic glasses with tunable liquid-crystalline order. *Physical review letters* **2018**, *120* (5), 055502.
- (6) Chen, Z.; Yu, J.; Teerakapibal, R.; Meerpoel, L.; Richert, R.; Yu, L. Organic glasses with tunable liquid-crystalline order through kinetic arrest of end-over-end rotation: the case of saperconazole. *Soft Matter* **2020**, *16* (8), 2025-2030.
- (7) Chen, Z.; Bishop, C.; Thoms, E.; Bock, H.; Ediger, M. D.; Richert, R.; Yu, L. Controlling the Columnar Order in a Discotic Liquid Crystal by Kinetic Arrest of Disc Tumbling. *Chemistry of Materials* **2021**, *33* (12), 4757-4764.
- (8) Tarnacka, M.; Adrjanowicz, K.; Kaminska, E.; Kaminski, K.; Grzybowska, K.; Kolodziejczyk, K.; Wlodarczyk, P.; Hawelek, L.; Garbacz, G.; Kocot, A. Molecular dynamics of itraconazole at ambient and high pressure. *Physical Chemistry Chemical Physics* **2013**, *15* (47), 20742-20752.
- (9) Yu, J.; Chen, Z.; Teerakapibal, R.; Benmore, C.; Richert, R.; Yu, L. Structures of glasses created by multiple kinetic arrests. *The Journal of Chemical Physics* **2022**, *156* (8), 084504.
- (10) Schönhals, A.; Zubowa, H. L.; Fricke, R.; Frunza, S.; Frunza, L.; Moldovan, R. On the Dielectric Behavior of Unaligned Samples of 4-n-Octyl-4'-cyanobiphenyl (8CB). *Crystal Research and Technology: Journal of Experimental and Industrial Crystallography* **1999**, *34* (10), 1309-1314.
- (11) Brás, A.; Dionísio, M.; Huth, H.; Schick, C.; Schönhals, A. f of glassy dynamics in a liquid crystal studied by broadband dielectric and specific heat spectroscopy. *Physical Review E* **2007**, *75* (6), 061708.
- (12) Elmahdy, M.; Floudas, G.; Mondeshki, M.; Spiess, H. W.; Dou, X.; Müllen, K. Origin of the complex molecular dynamics in functionalized discotic liquid crystals. *Physical review letters* **2008**, *100* (10), 107801.

- (13) Hansen, M.; Feng, X.; Macho, V.; Müllen, K.; Spiess, H. W.; Floudas, G. Fast and slow dynamics in a discotic liquid crystal with regions of columnar order and disorder. *Physical Review Letters* **2011**, *107* (25). 257801.
- (14) Yildirim, A.; Kolmangadi, M. A.; Bühlmeyer, A.; Huber, P.; Laschat, S.; Schönhals, A. Electrical conductivity and multiple glassy dynamics of crown ether-based columnar liquid crystals. *The journal of physical chemistry B* **2020**, *124* (39), 8728-8739.
- (15) Yildirim, A.; Krause, C.; Zorn, R.; Lohstroh, W.; Schneider, G. J.; Zamponi, M.; Holderer, O.; Frick, B.; Schönhals, A. Complex molecular dynamics of a symmetric model discotic liquid crystal revealed by broadband dielectric, thermal and neutron spectroscopy. *Soft matter* **2020**, *16* (8), 2005-2016.
- (16) Yildirim, A.; Krause, C.; Huber, P.; Schönhals, A. Multiple glassy dynamics of a homologous series of triphenylene-based columnar liquid crystals—A study by broadband dielectric spectroscopy and advanced calorimetry. *Journal of Molecular Liquids* **2022**, *358*, 119212.
- (17) Feng, X.; Marcon, V.; Pisula, W.; Hansen, M. R.; Kirkpatrick, J.; Grozema, F.; Andrienko, D.; Kremer, K.; Müllen, K. Towards high charge-carrier mobilities by rational design of the shape and periphery of discotics. *Nature materials* **2009**, *8* (5), 421-426.
- (18) Pisula, W.; Zorn, M.; Chang, J. Y.; Müllen, K.; Zentel, R. Liquid crystalline ordering and charge transport in semiconducting materials. *Macromolecular rapid communications* **2009**, *30* (14), 1179-1202.
- (19) Kaafarani, B. R. Discotic liquid crystals for opto-electronic applications. *Chemistry of Materials* **2011**, 23 (3), 378-396.
- (20) O'Neill, M.; Kelly, S. M. Ordered materials for organic electronics and photonics. *Advanced Materials* **2011**, *23* (5), 566-584.
- (21) Kelber, J.; Achard, M. F.; Durola, F.; Bock, H. Distorted Arene Core Allows Room-Temperature Columnar Liquid-Crystal Glass with Minimal Side Chains. *Angewandte Chemie International Edition* **2012**, *51* (21), 5200-5203.
- (22) Boden, N.; Bushby, R.; Clements, J. Electron transport along molecular stacks in discotic liquid crystals. *Journal of Materials Science: Materials in Electronics* **1994**, *5*, 83-88.
- (23) García-Frutos, E. M.; Pandey, U. K.; Termine, R.; Omenat, A.; Barberá, J.; Serrano, J. L.; Golemme, A.; Gómez-Lor, B. High Charge Mobility in Discotic Liquid-Crystalline Triindoles: Just a Core Business? *Angewandte Chemie* **2011**, *123* (32), 7537-7540.
- (24) Heiney, P. A. Datasqueeze: A software tool for powder and small-angle X-ray diffraction analysis. *Newsletter of the IUCr Commission on Powder Diffraction* **2005**, *32*, 9-11.
- (25) Prasad, S. K.; Rao, D. S.; Chandrasekhar, S.; Kumar, S. X-Ray studies on the columnar structures of discotic liquid crystals. *Molecular Crystals and Liquid Crystals* **2003**, *396* (1), 121-139.
- (26) McMillan, W. L. Simple molecular model for the smectic A phase of liquid crystals. *Physical Review A* **1971**, *4* (3), 1238.
- (27) McMillan, W. X-ray scattering from liquid crystals. I. Cholesteryl nonanoate and myristate. *Physical Review A* **1972**, *6* (3), 936.
- (28) Fontes, E.; Heiney, P. A.; Ohba, M.; Haseltine, J. N.; Smith III, A. B. Molecular disorder in columnar-phase discotic liquid-crystal strands. *Physical Review A* **1988**, *37* (4), 1329.
- (29) Chen, Z.; Huang, C.; Yao, X.; Benmore, C. J.; Yu, L. Structures of glass-forming liquids by x-ray scattering: Glycerol, xylitol, and D-sorbitol. *The Journal of Chemical Physics* **2021**, *155* (24), 244508.
- (30) Simon, S.; Sobieski, J.; Plazek, D. Volume and enthalpy recovery of polystyrene. *Polymer* **2001**, *42* (6), 2555-2567.
- (31) Möller, M.; Wendorff, J.; Werth, M.; Spiess, H. W. The nature of the glass transition in a columnar hexagonal ordered phase. *Journal of non-crystalline solids* **1994**, *170* (3), 295-299.
- (32) Wang, L.-M.; Tian, Y.; Liu, R.; Richert, R. Calorimetric versus kinetic glass transitions in viscous monohydroxy alcohols. *The Journal of chemical physics* **2008**, *128* (8), 084503.

- (33) Bishop, C.; Chen, Z.; Toney, M. F.; Bock, H.; Yu, L.; Ediger, M. Using Deposition Rate and Substrate Temperature to Manipulate Liquid Crystal-Like Order in a Vapor-Deposited Hexagonal Columnar Glass. *The Journal of Physical Chemistry B* **2021**, *125* (10), 2761-2770.
- (34) Bishop, C.; Bagchi, K.; Toney, M. F.; Ediger, M. Vapor deposition rate modifies anisotropic glassy structure of an anthracene-based organic semiconductor. *The Journal of Chemical Physics* **2022**, *156* (1), 014504.
- (35) Seddon, J. M. Structural studies of liquid crystals by X-ray diffraction. *Handbook of liquid crystals* **1998**, *1*, 635-679.